

# Investigations of Calcium Aluminate Slag Penetration to MgO Monolithic Refractories in Steelmaking Process

M. H. Amin<sup>1\*</sup>, A. Kazemzadeh<sup>2</sup>, B. Arfaei<sup>3</sup>, N. Saha-Chaudhury<sup>4</sup> and V. Sahajwalla<sup>5</sup>

1, 2- Material and Energy Research Center, P.O. Box 14155-4777 Tehran, Iran

3- Department of Mechanical Engineering, State University of New York, USA

4, 5- School of Materials Science and Engineering, UNSW, Sydney, Australia

Received March 6, 2007; Accepted November 28, 2007

---

## Abstract

In this study, slag penetration into a magnesia refractory monolithic was investigated by the crucible test method. A synthetic calcium aluminate slag system has been used to study commercial magnesia mix refractory for 1, 2, 3, 4, 5 and 6 hours at 1450°C and 1600°C.

It has been shown that the penetration rate is controlled by a diffusion mechanism at 1450°C. In this case, capillaries are the main channels of initial slag penetration into the refractory. In the penetration process of the slag system, calcium silicate was formed on the surfaces of MgO grains at 1450°C and around them by reaction between grain boundary and mayenite, as a main phase of slag with a low melting point.

Dissolution of the refractory components in the slag could be supported by the penetration process at 1600°C. In this case, dissolution of the refractory components in the slag not only makes new open channels, but also changes the local slag composition, resulting in an increase in surface tension and viscosity of the slag.

*Keywords:* Slag, Magnesia, Calcium aluminate slag, Crucible test method, Corrosion.

---

## 1. Introduction

In recent years, demand for clean steel has increased rapidly. The growing demand for high purity and cleanliness requires better control, and therefore a better understanding of the interactions of refractory with slag and steel in steelmaking process. Refractories lining of ladle and tundish cannot avoid contact between molten steel and slags. The interaction of refractories with their surroundings in high temperature industries remains as one of the major challenges. The materials must not only be stable at high temperatures but also withstand mechanical stresses, as well as corrosion resistance by liquids, metal and slags<sup>1</sup>.

The most significant trend in refractories technology in the last two decades has been the ever increasing use of monolithic (or unshaped) refractories such as those which now, in many countries, account for more than 50% of total production due to their quicker and cheaper installation, and properties approaching those of shaped (brick) refractories. Magnesia monolithics are unshaped refractories commonly used in steelmaking for the maintenance of tundishes. Therefore, a fundamental understanding of the dissolution behaviour of magnesia monolithic into molten slag is important in steelmaking<sup>2</sup>.

Many researchers have conducted experimental investigations of penetration and corrosion of magnesia monolithic by slags. These studies showed that the rate of slag penetration increases with increasing pore radius,<sup>2</sup> Al<sub>2</sub>O<sub>3</sub> and Fe concentration in the slag,<sup>2-5</sup> test temperature,<sup>2</sup> and with decreasing slag basicity (C/S ratio)<sup>2,4,6,7</sup> as a result of the high capability of dissolving magnesia in the slag<sup>4,6</sup>. Molnar et al. have studied the interaction of molten silicate and ferritic-calcium slags with magnesite refractories. They suggested that slags of the system FeO-Fe<sub>2</sub>O<sub>3</sub>-CaO penetrate more readily beneath the surface of the refractories than the silicate slags, but show lower chemical aggressivity<sup>8</sup>. The effect of the slag type on penetration and corrosion resistance of high purity sintered and fused magnesia has been reported by Zhang et al.<sup>7</sup> Some researchers have shown that reaction between CaO in slag and Al<sub>2</sub>O<sub>3</sub> in the monolithic makes low-melting calcium aluminates, while reaction between CaO in slag and Al<sub>2</sub>O<sub>3</sub> in brick results in the formation of spinel at the slag/grain interface<sup>9,10</sup>. As a result, MgO bricks have higher slag resistance than the

---

\*Corresponding author:

Tel: +98-261-6204130-9 Fax: +98-261-6201888

E-mail: m-amin@merc.ac.ir

Address: Material and Energy Research Center,

P. O. Box 14155-4777 Tehran, Iran

---

1- Assistant Professor, Material and Energy Research Center

2- Assistant Professor, Material and Energy Research Center

3- PhD Student, Department of Mechanical Engineering, State University of New York

4- Member of Faculty, School of Materials Science and Engineering, UNSW

5- Professor, School of Materials Science and Engineering, UNSW

MgO Monolithics<sup>9)</sup>. The penetration and corrosion mechanisms of magnesia monolithic by silicate slags were investigated<sup>5)</sup>. Firstly, the slag, as a single liquid phase, penetrated the monolithic via the open pores; secondly, the penetrating slag reacted with the surrounding MgO; and finally, the ions (e.g. Ca and Fe) from the slag penetrated more deeply via diffusion processes<sup>5)</sup>. Yu et al. suggested that the penetration rate of slag into the refractory is related to the corrosion rate<sup>11)</sup>. Studies reported in the literature have shown that interactions between slag and refractory materials are dependent on both the slag composition and the type of refractory material.

The corrosion process could be defined as any type of interaction between a solid phase and a fluid phase that results in a deleterious effect on either of the phases. The corrosion of the refractory is a very complex phenomenon involving not only chemical wear (corrosion) but also physical/mechanical wear (such as erosion/abrasion) processes, which may act synergistically. Corrosion of the lining material in contact with slag is usually described on the basis of the following phenomena: dissolution, which is a chemical process by which the refractory materials are continuously dissolved; and penetration, by which the slag penetrates into the refractory and causes erosion, which is the abrasion process of the refractory material exposed to slag movement.

There exist many reports on the corrosion of magnesia refractories by various slags<sup>3,7,10,12,13)</sup> and studies have been conducted to investigate metal/MgO refractory interactions in steelmaking<sup>14-20)</sup>.

Despite these studies, the penetration and corrosion mechanism of commercial magnesia monolithic by calcium aluminate slags have not yet been studied. In the present work, a synthetic calcium aluminate slag system has been used to study corrosion of commercial magnesia mix refractory for various temperatures and times. The investigation is worthwhile, because corrosion of these materials usually occurs in contact with synthetic slag that is carried over from the ladle, and there are still some obscure points concerning the relevant parameters which may influence this problem. This problem generally dominates the refractory life, and it is necessary to apprehend its mechanism.

## 2. Experimental Details

The corrosion of commercial magnesia refractory by calcium aluminate slag was studied using a static crucible corrosion test, with a fixed amount (50g) of powder slag placed in each crucible. Table 1 shows the chemical composition of the magnesia mix. The slag mixtures of fixed composition were prepared by weighing 173.16g reagent grade calcium carbonate (CaCO<sub>3</sub>) and 157.57g aluminum

hydroxide (Al(OH)<sub>3</sub>), wet-mixing them with ethanol in an alumina ball mill for 3h and drying at 120°C for 24h.

The test crucibles were prepared by drilling a hole 10cm diameter × 7cm deep cup cut out of high alumina brick and then lining them (to 20mm thickness) with the magnesia monolithic powder mixed with 10 wt% of water, by patching. In this case, there is a condition the same as the situation of a magnesia monolithic powder mixed lining on high alumina brick working layer of tundishes, which are used in Mobarakeh Steel Plant. A schematic figure of the crucible is shown in Figure 1.

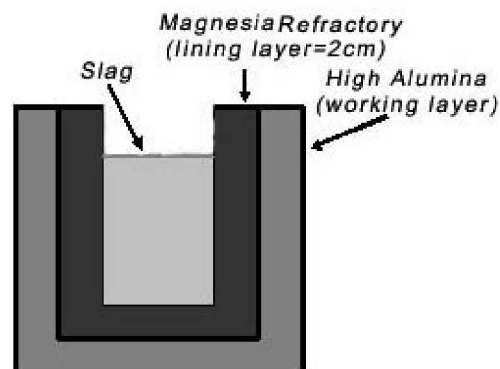


Fig. 1. Schematic figure of crucible.

The slag was melted in a Pt crucible at 1650°C for 3h and monolithic crucibles were heated at 1200°C for the same length of time. The slag then was poured into the magnesia crucible inside the furnace immediately. The slag penetration was carried out in the furnace in air atmosphere at 1450°C and 1600°C for 1, 2, 3, 4, 5 and 6hour. After holding each crucible for a specified fixed time, it was taken out of the furnace and cooled by blowing cold air from just above the crucible for 1h. To study the microstructure and phase analysis in the monolithic without slag present, we fired one sample following the same heating program used for the corrosion test.

The slag penetration was determined on a cut face of the crucible mounted in epoxy resin. Chemical analyses were performed using X-ray fluorescence spectrometer (ARL XRF). An X-ray diffraction technique was used to identify phase changes using a Philips-112 X-ray diffractometer, in the angle range 5 to 80° with a step size of 0.02°. The cross-section of the used lining was examined by optical microscopy (Zeiss Oxio-Vert 200) and the observation of microstructure was performed on polished faces using a scanning electron microscope (SEM) equipped with X-ray spectroscopy (LEO 460). The apparent porosity and density were determined according to ASTM C20-87. The pore size distribution was determined by a mercury porosimeter according to DIN EN 993.

Table 1. Chemical composition of monolithic.

Oxide	MgO	CaO	SiO <sub>2</sub>	Fe <sub>2</sub> O <sub>3</sub>	Al <sub>2</sub> O <sub>3</sub>	K <sub>2</sub> O	Na <sub>2</sub> O
Mass%	95.32	1.53	2.43	0.11	0.08	0.10	0.43

### 3. Experimental Results

#### 3.1. Characterization of Refractory and Slag

The apparent porosity, bulk density and the average pore radius of the samples after drying were 8.4%, 2.96g/cm<sup>3</sup> and 0.15 micron, respectively.

XRD patterns of magnesia monolithic and synthesized slag are shown in Figures 2 and 3, respectively. The main phase of the monolithic sample is MgO periclase. In addition to the MgO main peak, weak peaks also exist in the XRD pattern which are attributed to monticellite (CaO.MgO.SiO<sub>2</sub>). The  $\frac{CaO}{SiO_2}$  ratio of the used magnesia

monolithic was less than 1. According to references, monticellite (CMS), forsterite (2MgO.SiO<sub>2</sub>) and magnesiumferrite (MgO.Fe<sub>2</sub>O<sub>3</sub>) would be expected in addition to periclase under these conditions<sup>21,22</sup>. However, X-ray diffraction indicates only the presence of monticellite while forsterite and magnesiumferrite can not be identified.

Mayenite is the main phase of the slag sample in Figure 3, which matches with the XRD pattern in PDF 9-0413 reference card with chemical formula of Ca<sub>12</sub>Al<sub>14</sub>O<sub>33</sub>(melting point, 1415°C). In addition to the main phase, other weak peaks are also observed which are attributed to calcium aluminium oxide (3CaO.Al<sub>2</sub>O<sub>3</sub>) with melting point 1900°C, which matches with the XRD patterns in PDF 8-0005 and 6-0495 reference cards.

#### 3.2. Microstructure and Phase Analysis

A backscattered electron image of the fired magnesia monolithic microstructure before slag penetration is shown in Figure 4. It was observed that a grain boundary phase wetted the MgO grains. Figure 5(a) shows the typical elemental analysis pattern of the boundary phase among the periclase particles, and the mean of the results is shown in Table 2. It is shown by X-ray diffraction that the main grain boundary phase is based on monticellite. This phase is the most undesirable phase because of its low melting point (about 1480°C) which decreases the refractoriness of the product<sup>23, 24</sup>. The data in Table 2 confirm that these phases have similar stoichiometric compositions of monticellite accompanying forsterite. This could be due to dissolution of some forsterite in monticellite and vice versa<sup>25</sup>. Apart from MgO and monticellite, there is a bright phase present in the microstructure. Figure 5(b) shows the typical elemental analysis pattern of this phase. According to references,<sup>22</sup> this phase could be magnesiumferrite (melting point, 1750°C) with higher atomic number to appear as a lump pocket due to low solubility of this phase in monticellite.

Table 2. Elemental analysis of secondary phases in the fired magnesia monolithic.

Element	Mg	Ca	Si
Mol%	15.47	13.16	14.24

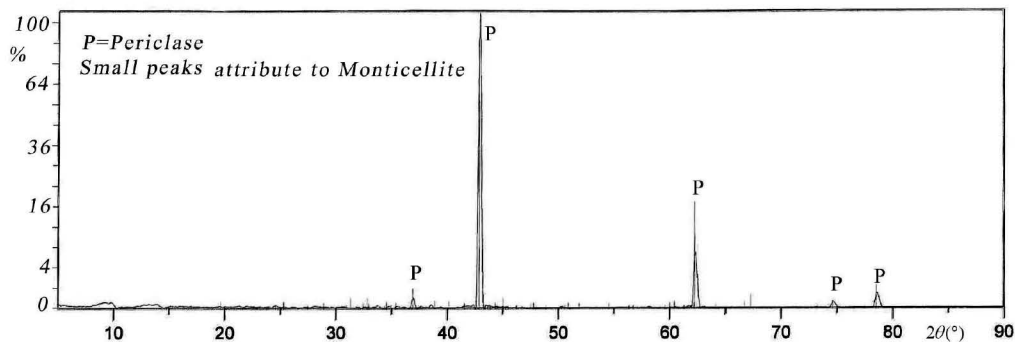


Fig. 2. Partial XRD pattern of magnesia monolithic.

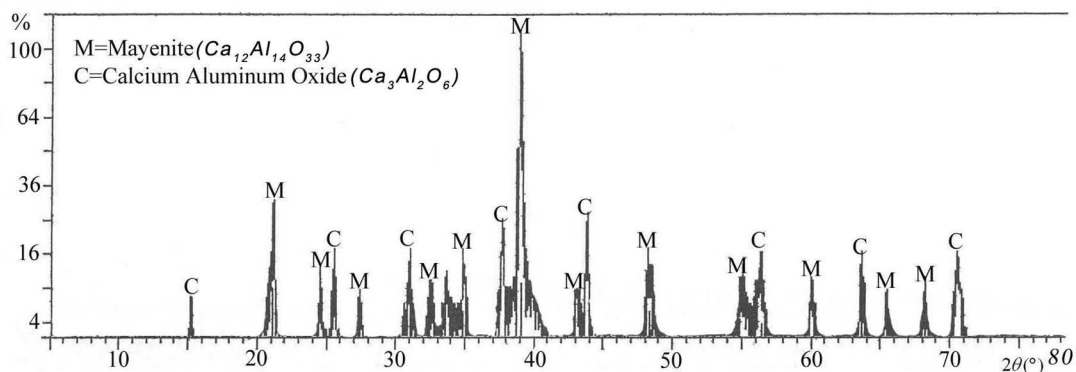


Fig. 3. Partial XRD pattern of synthesized slag.

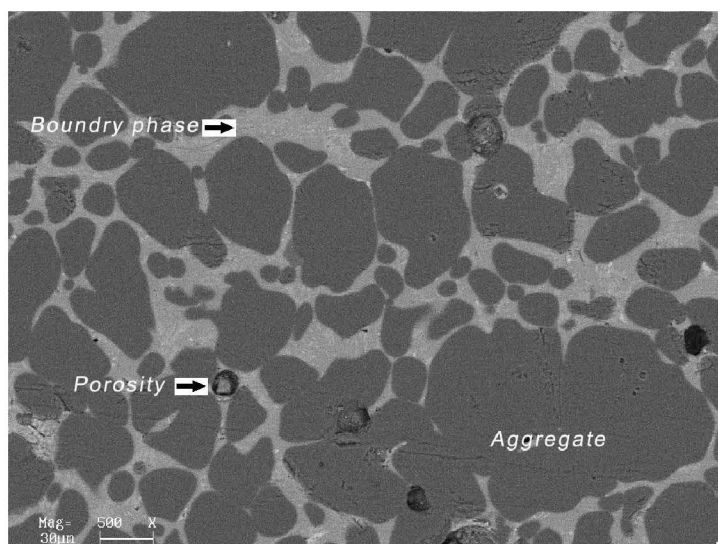


Fig. 4. SEM micrograph of the fired magnesia monolithic microstructure before penetration.

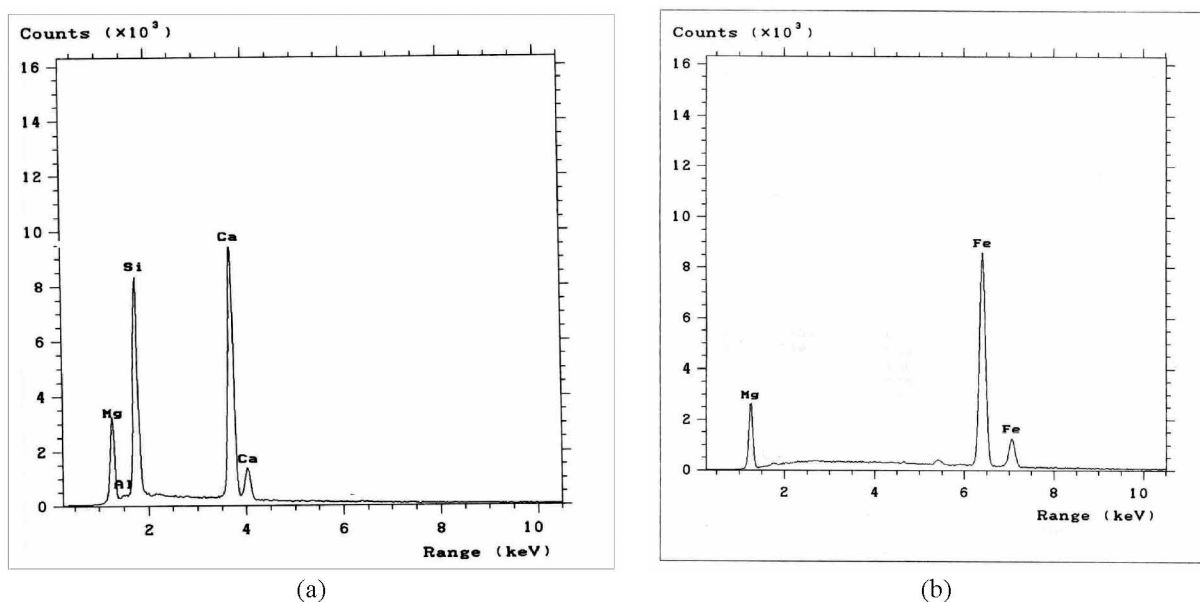


Fig. 5. X-ray spectroscopy of (a) the main grain boundary phase and (b) bright phase in the fired magnesia monolithic microstructure before penetration.

### 3.3. Slag Penetration into refractory

The relationships between penetration time and thickness of penetrated slag in the monolithic crucible at different temperatures are shown in Figure 6. The curve for the temperature of 1450°C was a parabolic curve; whereas the curve representing data at the temperature of 1600°C was linear (the correlation coefficient is equal to 1). A plot of thickness of penetrated slag in the monolithic crucible,  $h$ , against  $\sqrt{\text{time}}$  for samples at 1450°C (shown in Figure 7) indicates a good linear relationship, thus confirming the parabolic behaviour. The corrosion rate at 1600°C was faster than that at the lower temperature, since at this temperature, slag

penetrates throughout the whole magnesia monolithic lining just after 4 hours and reaches the high alumina brick working layer.

## 4. Discussion

### 4.1. Penetration Rate of Slag

Two distinct slopes indicate that the penetration of magnesia monolithic with calcium aluminate slag could be dictated by different mechanisms at the two temperatures. The parabolic curve is a sign that the penetration rate at 1450°C is controlled by a diffusion mechanism. In this case, the rate equation could be as follows:

$$h^2 = k't \quad \text{or} \quad h = k\sqrt{t} \quad (1)$$

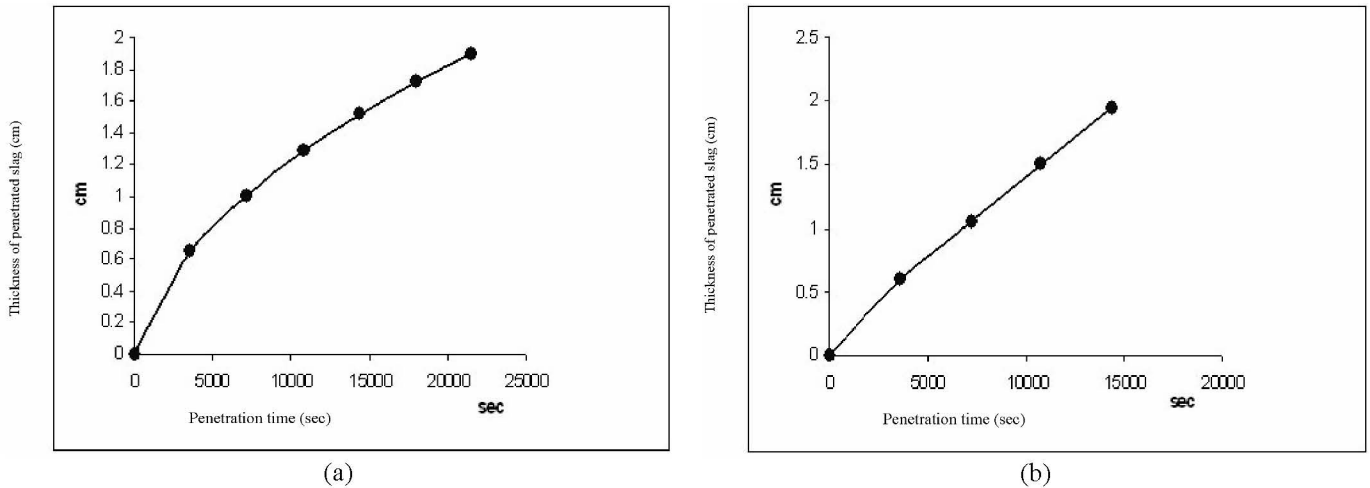


Fig. 6. Relation between penetration time (sec) and thickness of penetrated slag (cm) in the monolithic crucible at (a) 1450°C and (b) 1600°C.

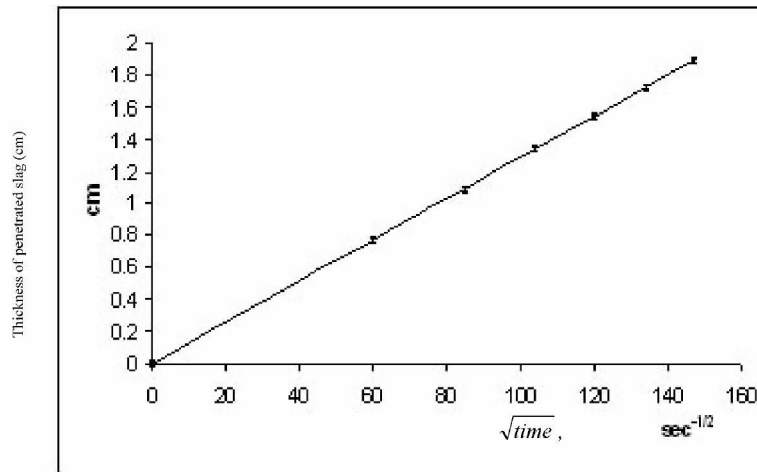


Fig. 7. Relation between thickness of penetrated slag ( $h$ ) and  $\sqrt{\text{time}}$  at 1450°C.

where  $h$  is the slag penetration depth (cm),  $t$  is time (sec) and  $k'$  ( $\text{cm}^2\text{sec}^{-1}$ ) and  $k$  ( $\text{cm}\cdot\text{sec}^{-1/2}$ ) are rate constant of penetration. A plot of  $h$  against  $\sqrt{\text{time}}$ , shown in Figure 7, indicates a good linear relationship and yields an overall rate constant of  $0.013 \text{ cm}\cdot\text{sec}^{-1/2}$ .

Capillaries, such as open pores and microcracks, are the main channels of initial slag penetration into a refractory. In this case, the penetration rate  $dh/dt$  of slag into a capillary can be expressed by Poiseuille's law<sup>1)</sup>:

$$\frac{dh}{dt} = \frac{r^2 \Delta P}{8\eta h} \quad (2)$$

where  $r$  is the capillary radius,  $\Delta P$  the capillary sucking pressure and  $\eta$  is viscosity of the slag. The term  $\Delta P$  is expressed by

$$\Delta P = 2\gamma \cos \theta / r \quad (3)$$

where  $\gamma$  is the slag surface tension and  $\theta$  the wetting or contact angle. By eliminating  $\Delta P$  from equation (2):

$$\int_0^t h dh = \frac{r^2 \gamma \cos \theta}{4\eta} \int_0^t \frac{1}{h} dt \quad \text{So: } h^2 = \frac{r^2 \gamma \cos \theta}{2\eta} t \quad (4)$$

Comparison between equations (1) and (4) gives the rate constant of penetration as follows:

$$k = \sqrt{\frac{r^2 \gamma \cos \theta}{2\eta}} \quad (5)$$

#### 4.2. Slag Viscosity and Surface Tension

Most models for calculating viscosity are based on numeric adjustments starting from experimental data, and are rarely based on the slag structure<sup>26)</sup>. The Urbain model estimates the viscosity of slags as a function of chemical composition and mineralogical nature<sup>26)</sup>. This model describes temperature dependence of the slag viscosity ( $\eta$ ) using the Weymann equation<sup>10)</sup>:

$$\eta (\text{Ns} / \text{m}^2) = 0.1QT \exp\left(\frac{1000P}{T}\right) \quad (6)$$

where  $T$  is the absolute temperature, and  $P$  and  $Q$  are constants obtained by the following equations<sup>10)</sup>:

$$Q = \exp(-11.6725 - 0.263P) \quad (7)$$

$$P = P_0 + P_1N + P_2N^2 + P_3N^3 \quad (8)$$

$$P_0 = 13.8 + 39.9355\alpha - 44.049\alpha^2 \quad (9)$$

$$P_1 = 30.481 - 117.1505\alpha - 129.9978\alpha^2 \quad (10)$$

$$P_2 = 40.9429 + 234.0486\alpha - 300.04\alpha^2 \quad (11)$$

$$P_3 = 60.7619 - 153.9276\alpha + 211.1616\alpha^2 \quad (12)$$

N is the mole fraction of SiO<sub>2</sub> in the slag and α is the mole fraction of CaO+MgO/CaO+MgO+Al<sub>2</sub>O<sub>3</sub> in the slag. In this study, α is 0.63; therefore slag viscosity can be expressed by following equation:

$$\eta(Ns/m^2) = 3.02 \times 10^{-9} T \exp\left(\frac{21451.63}{T}\right) \quad (13)$$

The viscosity values of the original slag at temperatures of 1450°C and 1600°C are 1.33 and 0.53 Ns/m<sup>2</sup>, respectively. It was found that the viscosity of the liquid phase decreased with increasing temperature. Thus, the rate constant of penetration increased accordingly.

The surface tension, γ, of the slag was calculated by the following equation:<sup>10)</sup>

$$\gamma(N/m) = (\mu_{Si}F_{Si} + \mu_{Al}F_{Al} + \mu_{Ca}F_{Ca} + \mu_{Mg}F_{Mg}) \quad (14)$$

In the above equation, μ is the mole fraction of a cation of an oxide component. The mole fraction of cations in the original slag is 0.00, 0.54, 0.46 and 0.00 for cations of Si, Al, Ca and Mg, respectively. F is the constant known as the surface tension factor of a cation of an oxide component. This factor is 0.34, 0.34, 0.47 and 0.58 for cations of Si, Al, Ca and Mg, respectively<sup>10)</sup>. Therefore, the surface tension, γ, of the original slag was calculated as 0.3998 N/m.

### 4.3. Slag Penetration Phenomenon and Associated Mechanism

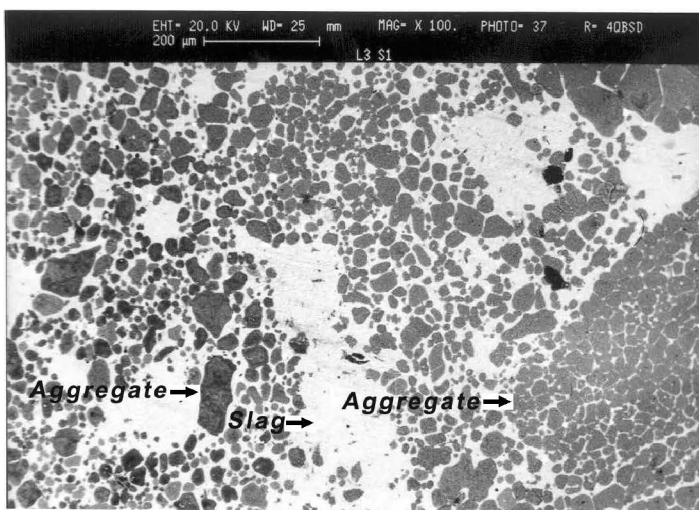
The average pore radius was about 1.5×10<sup>-7</sup>m

and the viscosity of the original slag at a temperature of 1450°C is 1.33 Ns/m<sup>2</sup> or 13.3 Poise, also assuming θ << 90° for basic slags, thus cos θ ≈ 1,<sup>27)</sup> and the rate constant gives: (15)

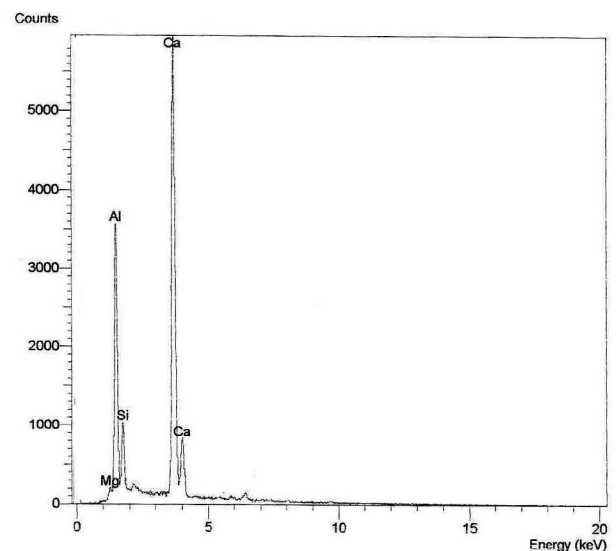
$$k = \sqrt{\frac{0.3998Nm^{-1} \times 1.5 \times 10^{-7}m}{2 \times 1.33N.Sec.m^{-2}}} = 1.50 \times 10^{-4} m.sec^{-1/2} = 0.015cm.sec^{-1/2}$$

There is a small difference between the calculated rate constant and experimental rate constant. The infiltration rate is affected by the temperature gradient in the refractory. When the temperature decreases, the viscosity increases, so in fact, the experimental rate constant decreases.

Slag temperature has a large effect on the penetration depth through its effect on η. Clearly, what is missing from equation (5) is a factor describing the microstructure of a refractory, although this can be incorporated in the r term. Figure 8 shows the backscattered electron image of the refractory matrix in the crucible, after slag reaction at 1450°C for 6 hour, along with the typical elemental analysis pattern of the boundary phase among the periclase particles. It is evident that the main bright colour phase is based on calcium aluminate. It was observed that the MgO grain boundaries were corroded by slag penetration. The image in Fig.8 also shows the degree to which MgO grains were isolated in the slag. It was confirmed by XRD analysis that the corroded sample had calcium aluminate phases co-existing with periclase. Figure 9 shows the XRD pattern of the sample taken from the slag-penetrated portion of the monolithic crucible, after slag reaction at 1450°C for 6 hours. The diffraction pattern showed the presence of periclase, mayenite and dicalcium silicate (PDF 3-0753).



(a)



(b)

Fig. 8. (a) SEM micrograph of slag-penetrated portion of the monolithic crucible, after slag reaction at 1450°C for 6 hour and (b) X-ray spectroscopy of the bright phase.

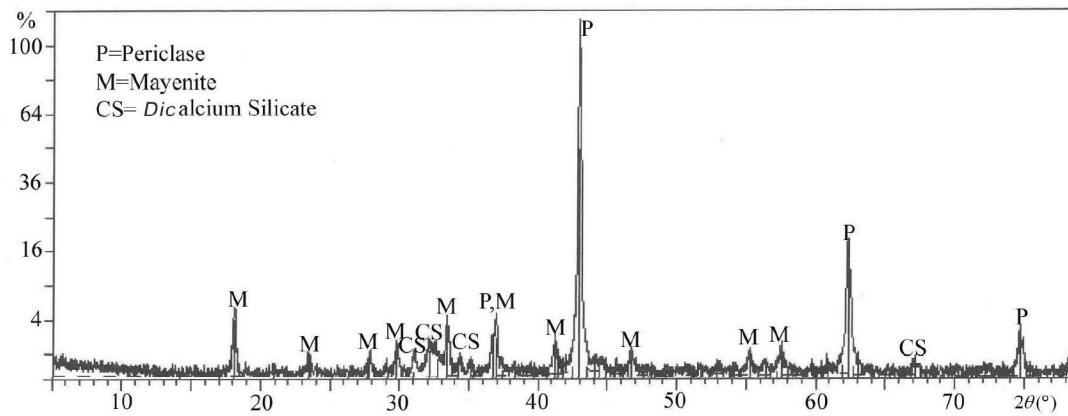


Fig. 9. Partial XRD pattern of corroded samples.

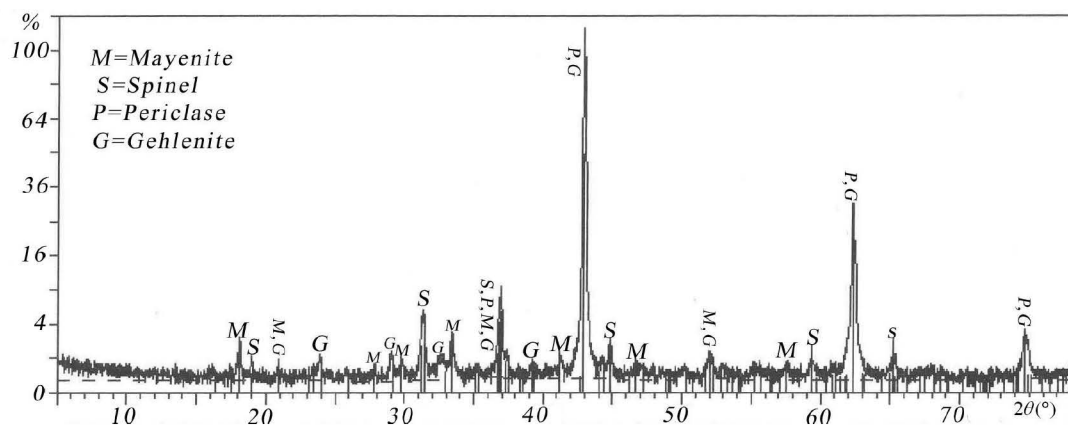


Fig. 10. XRD patterns of slag in the surface of refractory after corrosion test at 1600 °C.

From equation (5) it can be seen that at higher temperatures, the penetration rate increases with decreasing slag viscosity. It is this relation which means that on first contacting the hot surface liquid, slag penetrates by capillary or wetting suction to depth  $h$  down open pores of radius  $r$ , dependent in large part on the temperature of the refractory. As temperature decreases away from the hot phase, slag viscosity increases, so the slag is too viscous to penetrate further.

As shown in Figure 6 (b), a plot of the thickness of penetrated slag in the monolithic crucible ( $h$ ) against time (second) at a temperature of 1600°C was linear (because the correlation coefficient is equal to 0.998)<sup>28</sup>. Examination of slag in the corroded sample at 1600°C by XRD has shown the dissolution of the refractory components in the slag. As apparent from Figure 10, the XRD patterns of slag in the surface of the refractory after a corrosion test at 1600°C show the existence of both periclase (MgO) and spinel  $MgAl_2O_4$  (PDF 5-0672) accompanying calcium aluminate slag. In addition, the diffraction pattern also showed the weak peaks that indicate gehlenite compound ( $2CaO \cdot Al_2O_3 \cdot SiO_2$ , refer to PDF card 35-0755). The existence of silicate phase in slag indicates that corrosion of the MgO monolithic by

calcium aluminate slag was related to the dissolution of both MgO and monticellite ( $CaO \cdot MgO \cdot SiO_2$ ). In this case, the mechanism is as follows. MgO in the monolithic reacted with  $Al_2O_3$  to form spinel and CMS in the monolithic (mainly in the matrix) reacted with calcium aluminate from the slag diffused to the monolithic, to form  $2CaO \cdot Al_2O_3 \cdot SiO_2$  (melting point, 1593°C)<sup>29</sup>, and thus dissolved in the slag. The melting point of monticellite is 1488°C, so it should be solid phase at 1450°C but a liquid phase at 1600°C which would dissolve quickly in the local slag. As a result, it can be concluded that with increase in temperature, dissolution of refractory into slag leads to a deviation of the mechanism from diffusion.

Dissolution at refractory / slag interfaces is governed by (a) chemical reaction (or solution) at the interface, or (b) transport (or diffusion) of reacting species through the liquid boundary layer. Direct dissolution can be reaction or interface controlled when the diffusivity of reaction product is faster than the rate of chemical reaction at the interface. In this case the dissolution process may be directly controlled by a reaction that is of first order with respect to a reactant species. Dissolution of the refractory components, making new open channels

(e.g., by connecting some closed pores) leads to further penetration. In this case, the slag as a liquid phase, is driven into the refractory by the capillaries<sup>1)</sup>.

Dissolution of the refractory components in the slag not only makes new open channels, but also changes the local slag composition, and therefore, the slag viscosity and surface tension. The application of the Urbain model to estimate viscosity confirms that when the slag basicity increases, as dissolution of the MgO in slag occurs, viscosity decreases because MgO acts as a modifier<sup>26)</sup>. In addition, according to equations (6-12), the concentration of Al<sub>2</sub>O<sub>3</sub> in the liquid phase decreased by assuming that spinel was precipitated from the liquid phase (as shown in Figure 10) leading to an increase in the constant P.

Also, the surface tension of the liquid phase increased due to a decrease in the percentage of Al<sub>2</sub>O<sub>3</sub> having a small surface tension factor due to the precipitation of spinel, and an increase in the percentage of MgO having a large surface tension factor due to dissolution of MgO in the liquid phase. If the slag viscosity decreases or surface tension increases, then according to equation (5), it will accelerate the penetration.

From the above discussion, it is concluded that the slag penetration behaviour changed with increase in temperature conditions; the slag composition was changed by dissolution of MgO grains in slag, resulting in a decrease in viscosity and an increase in surface tension. The overall mechanism is schematically represented in Figure 11.

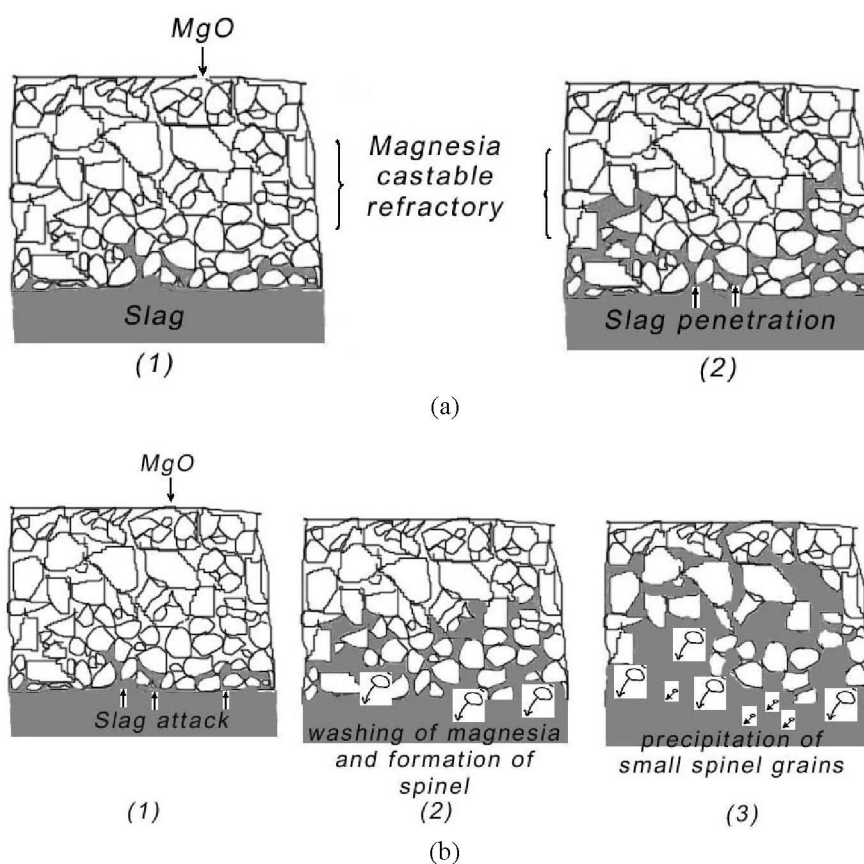


Fig. 11. Corrosion mechanism of magnesia refractory (a) at 1450°C and (b) at 1600°C.

## 5. Conclusions

Slag penetration studies at 1450°C and 1600°C were carried out using the crucible method in order to understand the mechanism of reaction between slag and the refractory, and the influence of reaction temperature on slag penetration into magnesia refractories. The following conclusions can be made from this study:

1- Penetration of magnesia monolithic refractory by calcium aluminate slag at 1450°C in a static test indicates that the corrosion rate is controlled by a diffusion mechanism. In this case, capillaries, such as open pores and microcracks, are the main channels of initial slag penetration into the refractory. In the penetration process of the slag system, calcium silicate was formed on the surfaces of MgO grains, and around them by reaction between



grain boundary and mayenite, as a main phase of slag with a low melting point.

2- As the test temperature increased, the corrosion mechanism of refractory by slag was changed, and the penetration rate at 1600°C was faster than at lower temperature. In this case, dissolution of the refractory components in the slag supported the penetration process. Consequently, dissolution of the refractory components in the slag not only makes new open channels, but also changes the local slag composition, resulting in a decrease in viscosity and an increase in surface tension of the slag. Accordingly, they lead to an increase in the penetration rate.

### Acknowledgments

The authors wish to acknowledge Mobarakeh Steel Plant (Isfahan, Iran) for the financial support of this project.

### References

- [1] W. E. Lee and S. Zhang; *International Materials Reviews*, 44 (1999), 77.
- [2] K. Mukai, Z. Tao, K. Goto, Z. Li, T. Takashima, *Refractories (Tokyo)*, 53(2001), 390.
- [3] P. Zhang and S. Seetharaman, *J. Am. Ceram. Soc.*, 77(1994), 970.
- [4] Z. Tao, K. Mukai, H. Yonezawa and Y. Yoshimura, *J. Tech. Assoc. Refract. Japan*, 20(2000), 10.
- [5] S. Zhang, W. E. Lee and N. Li, *Proc. of Conf. 'UNITECR '01', Unified Int. Tech. Conf. on Refractories.7th Biennial Worldwide Congress, Vol. 1, Cancun 4-7,( 2001)*, 65.
- [6] K. Matsu, F. Kawano and K. Nibu, *Refractories (Tokyo)*, 43(1991), 42.
- [7] S. Zhang, H. Sarpoolaky, N. J. Marriott and W. E. Lee, *British Ceramic Transactions*, 99(2000), 248.
- [8] L. Molnar, P. Vadasz and M. Kozlovsky, *Ceramics-Silikaty*, 37(1993), 121.
- [9] J-H. Woo, D-H. Kim and S-M. Kim, *Journal of the Korean Institute of Metals and Materials (South Korea)*, 39(2001), 835.
- [10] T. Matsui, K. Hiragushi, T. Ikemoto and K. Sawano, *J. Tech. Assoc. Refract. Japan*, 22(2002), 302.
- [11] Z. Yu, K. Mukai, K. Kawasaki and I. Furusato; *Journal of the Ceramic Society of Japan*, 101(1993), 533.
- [12] H. Fukuyama, J. R. Donald and J. M. Toguri, *J. Am. Ceram. Soc.*, 80(1997), 2229.
- [13] T. Matsui, K. Hiragushi, T. Ikemoto and K. Sawano, *Journal of the Technical Association of Refractories, Japan*, 23(2003), 11.
- [14] L. Zhao and V. Sahajwalla, *ISIJ International*, 43(2003), 1.
- [15] V. Sahajwalla, C. Wu, R. Khanna, N. S. Chaudhury and J. Spink; *ISIJ International*, 43(2003), 1309.
- [16] M. H. Amin, B. Arfaei and A. Kazemzadah; *Proc. of the 9<sup>th</sup> International Chemistry Conference in Africa, University of Dar Es Salaam, (2005)*, 14-SL18.
- [17] M. H. Amin, Z. Nemati and B. Akbari; *Proc. of the 5<sup>th</sup> Iranian Ceramic Congress, Iran University of Science and Technology Iran, (2004)*, 11.
- [18] M. H. Amin and B. Arfaei, *Proc. of the 5th European Continuous Casting Conference, Nice, France, (2005)*.
- [19] M. H. Amin and B. Arfaei, *Proc. of Iranian Steel Symposium 83, Iran Alloy Steel Co., (2005)*, 978.
- [20] M. H. Amin and N. Akbari, *Proc. of Iranian Steel Symposium 83, Iran Alloy Steel Co., (2005)*, 988 .
- [21] M. H. Amin, F. Golestanifard and F. Moztarzadah, *Industrial Ceramics*, 22(2002), 19.
- [22] T. Taschler, *Proc. of Tehran International Conference on Refractories, Iran (2004)*, 302.
- [23] M. H. Amin, *Industrial Ceramics*, 25(2005), 27.
- [24] M. H. Amin and F. Moztarzadah, *Journal of Faculty of Engineering (University of Tabriz), Iran*, 29(2004), 1.
- [25] M. H. Amin, F. A. Hessari and M. Solati, *Industrial Ceramics*, 23(2003), 205.
- [26] J. Madias, E. Brandaleze, M. Bentancour, R. Topolevsky and S. Camelli, *Proc. of Conf. 'UNITECR '01', Unified Int. Tech. Conf. on Refractories.7th Biennial Worldwide Congress, Vol. 1, Cancun, (2001)*, 475.
- [27] B. Sjodin, *Eldfasta Material, Technical Compendium, MEFOS, (1971)*.
- [28] Z. B. Alfassi, Z. Boger and Y. Ronen, *Statistical Treatment of Analytical Data, Blackwell publishing, CRC press, (2005)*.
- [29] W. S. Resende et al., *Journal of the European Ceramic Society*, 20(2000), 1419.